TESTING OF AGGREGATION MEASUREMENT TECHNIQUES FOR INTRAMEMBRANOUS PARTICLES

JOHN T. DONNELL II AND LEONARD X. FINEGOLD, *Department of Physics Drexel University Philadelphia, Pennsylvania 19104*

ABSTRACT Under various physiological and nonphysiological conditions, the intramembranous particles, as seen by freeze-fracture electron microscopy, may be in various degrees of aggregation. To compare various schemes for the measurement of the degree of aggregation, a computer program has been used to generate simulated aggregations. A simple and adequate technique for quantifying the degree of aggregation, which is practical for the electron microscopist, is presented.

INTRODUCTION

Freeze-fracture techniques have revealed various distributions of particles on the fracture surfaces of the membranes of cells (1). Under certain conditions, the particles appear to be aggregated. To understand better the mechanism of the clustering of the particles, one needs a (preferably simple) measure of the amount of aggregation in the sample electron micrographs under investigation. Several techniques for the comparison of states of aggregation have been attempted (2–8). A sample of tracings of electron micrographs showing particle aggregations, is shown in Fig. 1. With a simulation of the process of aggregation, it is possible to compare the merits of various quantification schemes. A program simulating the aggregation of particles was used to compare the various methods of measurement of the aggregation process. A simple, adequate, and practical technique, which can be performed by any electron microscopist, is described. The requirements of the technique are a small amount of computing time and a transparent ruled sheet.

The aggregation, in two dimensions, of distinct entities into larger groups is a widespread phenomenon, ranging from the scale of ecological systems (9), to membrane particle behavior. The latter small-scale phenomena are observed by electron microscopy where the membrane is viewed *en face*. Powerful techniques for observing the distribution, and the changes in the distribution, of labels on membranes include antibodies or lectins (2) conjugated to an electron-dense probe, and the freeze-fracture method by which intramembrane particles are observed (1). Although the treatment of this paper focuses on the aggregation of particles in the membrane, the methods are equally applicable to other situations in which the aggregation process is involved.

Although aggregation may be quite visible, meaningful measures of the degree of aggregation are difficult to find. Here, the results of a computer simulation are used, in which particles are moved in two dimensions and bound irreversibly upon their meeting at a certain prescribed binding distance, to generate simulated "electron micrographs" (Fig. 2). This

---

Dr. Donnell's current address is Information Services Group, Randolph, New Jersey 07869

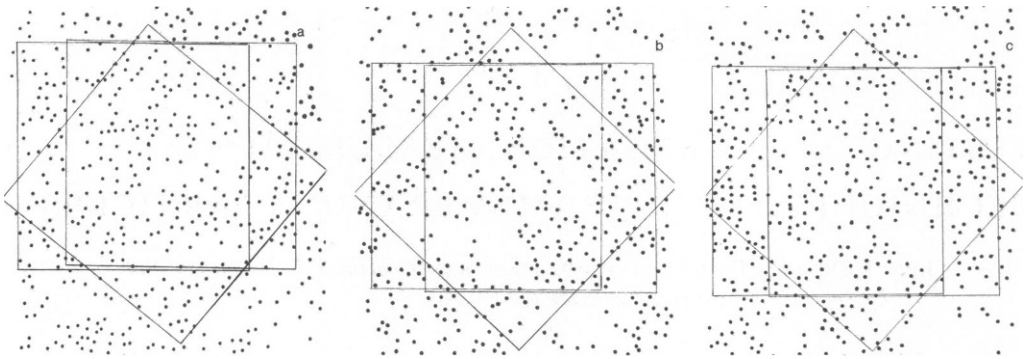

FIGURE 1 Aggregations of membrane particles. Tracings of three electron micrographs of freeze-cleavage of red blood cell ghost membranes are shown. Each tracing was overlaid with three grids at the locations indicated by the square outline to measure the degree of aggregation present.

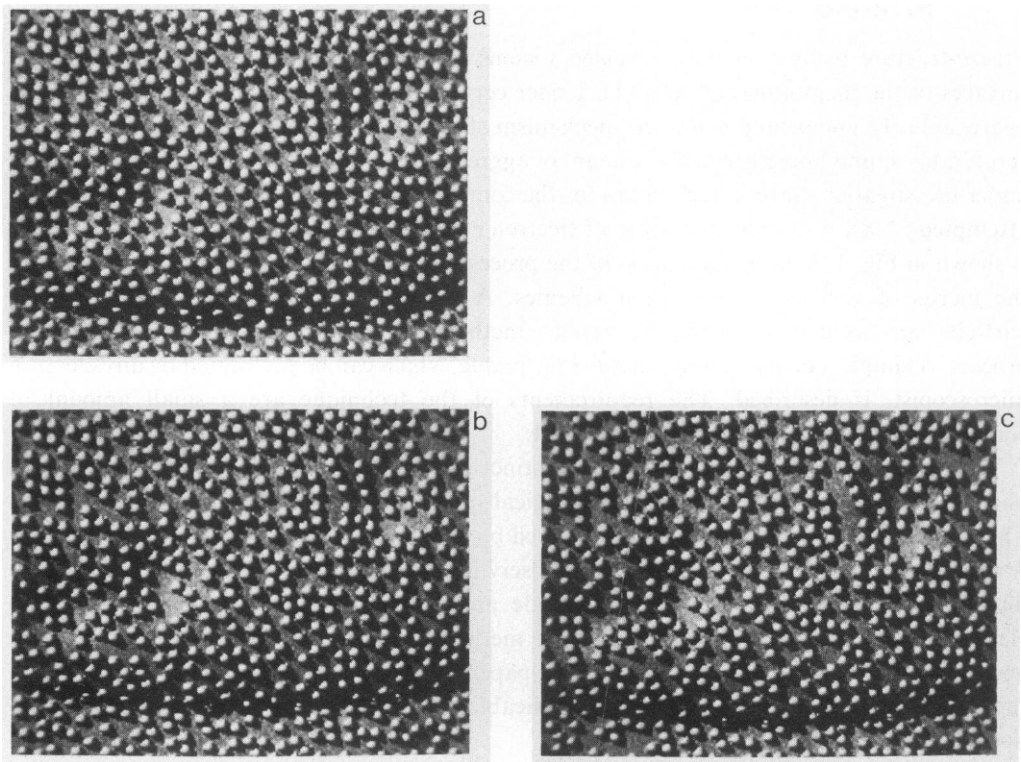

FIGURE 2 Simulated electron micrographs from the computer simulation program at a density of ρ = 0.0041 particles/nm^2. The three pictures are from a sequence of monotonically increasing aggregation. (*a*) is a random distribution of particles with no overlapping particles. (*b*) and (*c*) pictures were made as the aggregation progressed. The values for P, the aggregation parameter are 0.978, 1.706, and 3.817 for (*a*), (*b*), and (*c*), respectively.

approach is important because a set of pictures that correspond to the locations of simulated freeze-fracture particles at given times, is obtained, in which the particles continually and definitely aggregate in time. Hence, time can be used as a parameter, and any proposed measure of aggregation can be readily tested by observing whether it is monotonically increasing, i.e., never decreasing, with the time sequence of pictures. Any other separate parameter corresponding to an aggregation sequence requires laborious calculation. To use a naturally occurring sequence of aggregation pictures is not feasible, since the details of the aggregation process are not understood. The computer simulation was originally designed to simulate (10, 11) the fluid mosaic model of the membrane,[1] but here only the fact that it describes a process of monotonically increasing aggregation is used.

Four different methods of measuring the degree of aggregation were compared by using a computer simulation program to generate aggregation states. Since the behavior of the simulation program is known, the methods can be compared without preconception. Because the particles are only allowed to combine, and remain rigidly bound after collision, the size of the various clusters monotonically increases throughout the aggregation process. Therefore, it would be desirable for any aggregation measurement to exhibit the same sort of monotonically increasing behavior. For convenience, the degree of aggregation should be described by a single simple parameter. Subjective rankings of aggregation have been attempted (8), but an objective measurement of aggregation is difficult. An objective criterion for the comparison of aggregations would have obvious advantages over subjective determinations. When presented with an electron micrograph of an aggregation of freeze-fracture particles, an ideal apparatus would give one, or at most a few, parameters describing the aggregation.

A computer program (10, 11) is now available in which particles aggregate inexorably with time. The results of this computer simulation provide unique test material for any proposed scheme for the measurement of aggregation, and show that a "boxing" technique is the simplest useful measurement method. Hence, it is the method of choice.

SIMULATION OF AGGREGATION BY COMPUTER

Only a brief description of the aggregation program is given here (for greater detail see Donnell [10]), which is a refinement and optimization of an earlier version (11). The computer program for Monte Carlo simulation of the diffusion and binding of membrane particles in two dimensions creates the aggregation pictures or "states" which then are used in the comparison of the various aggregation measurement schemes. A state is defined as the relative spatial positions of the particles at a certain time, i.e., an instantaneous picture. Initially there are no bound particles, but as time passes clusters of particles are formed. Hence, each cluster begins as a cluster of one, i.e., a single particle. The particles are set up at time $t = 0$ in either of two ways: (*a*) a random arrangement with no particles overlapping or (*b*) a uniform square lattice arrangement. During each "machine cycle," i.e., between each producible picture, each cluster is moved randomly in turn. After each cluster movement the vicinity of each particle (say X) of the moved cluster is checked for the presence of other particles. If any allogeneic particles are found in the region near the particle X, the separation, S, between the particle X and the encountered particle from the allogeneic cluster is checked for the existence of a collision, i.e., $S < B$ (where B is a predetermined binding distance). If a

[1]S. I. Chan, private communication.

collision occurs the moved cluster is sent back along its original path until it just reaches the point where contact between the moved cluster and the contacted cluster is made, i.e., $S = B$, preserving the "hard-core" nature of the particles (10). When each cluster has been moved once and checked for collisions, the machine cycle is considered complete. The positions of the particles and the simulated time corresponding to that machine cycle are recorded for later use. It is these relative positions which are used for the comparisons of the various aggregation measurement methods. Sample aggregations generated by the computer are shown in Fig. 2. Nine runs of the computer program were made to compare the various aggregation measurement schemes: a key to explain their names is given in Table I.

METHODS FOR MEASUREMENT OF THE DEGREE OF AGGREGATION

Mean Cluster Size

First each cluster size and then the mean cluster size were determined. A particle is considered to be a part of a cluster when $S = B$, where S is the separation from at least one of the other members of the cluster, and where B is the given binding distance. Here, a value of 12.5 nm was used for the binding distance. A study of published freeze-fracture micrographs gives a peak in the radial distribution function at approximately 10 nm (12). For the calculation of the radial distribution function, it is necessary to know the exact positions of all the particles. Hence, if the method were to be used, it would be necessary to digitize (painfully) the coordinates of all of the particles. In general, an automatic or a convenient digitizing method would not be readily available to the electron microscopist.

Radial Distribution Function

The radial distribution function is determined by calculating the separation distance between each pair of particles, collecting all such distances, separating them into categories corresponding to small intervals of distance, determining the frequency distribution of the separation distances and then dividing the frequency for each category by the area of the annulus corresponding to that spacing. The radial distribution was used by Perelson (12) to show the local clustering of surface immunoglobin. It has also been used more recently in the analysis of intramembranous particles (13, 14). A plot of the resulting distribution of particles per unit area vs. separation distance is made. As with the previous method, it is necessary to digitize the coordinates of the particles.

Nearest-Neighbor Separations

In a square outward spiral search, the vicinity of each particle is scanned for the presence of other particles until 25 nearby particles are found. The search examines first the neighboring 8 square regions,

TABLE I
COMPUTER AGGREGATION SIMULATION RUNS

Name of run	Density	Seed	Starting arrangement
	Particles/nm²		
LDR	0.0021	27182818285	Random placed
LDS	0.0021	31415926536	Random placed
LDU	0.0021	27182818285	Uniform square
MDR	0.0032	27182818285	Random placed
MDS	0.0032	31415926536	Random placed
MDU	0.0032	27182818285	Uniform square
HDR	0.0043	27182818285	Random moved
HDS	0.0043	31415926536	Random moved
HDU	0.0043	27182818285	Uniform square

then the next 14 square regions, etc., until the first 25 particles are encountered. The separations of the particle from its six nearest neighbors were computed and kept for the average calculation. Averages of the nearest 2, 3, 4, 5, and 6 nearest neighbors for the particles were recorded.

Boxing Method

In the boxing method, the area of the electron micrograph of interest is divided into small "unit" boxes. The standard deviation, σ, of the number of particles per "scan" box, a grouping of $N \times N$ unit boxes, is used to compute σ_n, a normalized standard deviation. σ_n is then used as the measure of aggregation, $\sigma_n = \sigma/\sigma_r$, where σ_r is the standard deviation for a "random" arrangement of particles at the same density. Similar methods have been used to describe aggregations (2, 3).

This method involves the coarse digitization of the data. The exact coordinates of the particles are not needed. The sample area under investigation is divided into $L \times L$ square unit boxes. The number of boxes along a side, L, is chosen such that the diagonal of each is just smaller than B, the binding distance or the distance of closest approach of the particles under study. The choice of this box size limits the number of particle centers in any unit box to 1. Each of the unit boxes is given an integral pair of X and Y coordinates. The coordinates of each unit box containing the center of a particle are recorded rather than the exact coordinates of each particle. Hence, to make a measurement of the degree of aggregation of the particles in a given electron micrograph, one need construct only an overlay mesh to determine the box coordinates for each of the particles. Elaborate equipment for the digitizing of the data is no longer necessary—a simple rectangular grid drawn on a transparent sheet is sufficient. The data obtained is entered into the computer as integer coordinate pairs. The computer program, in effect, places a larger scan box of size $N \times N$ on the data, where N is the "mesh size," the number of unit boxes along the edge of the larger scan box. The number of occupied unit boxes in the scan box is counted for each possible location of the scan box within the mesh. The total number of samplings will then be $(L - N) \times (L - N) \times N \times N$. A count of the occupied unit boxes at each location of the scan box is made for mesh sizes from 2 to 10. The computer time required for the counting operation at each mesh size will vary approximately as N squared. The standard deviation for the number of occupied unit boxes, i.e., particle centers, in each possible scan box is computed as σ, where σ is given by

$$\sigma = \left\{ \frac{1}{(L-N)^2 - 1} \sum_{i=1}^{L-N} \sum_{j=1}^{L-N} \left[\frac{N^2 K}{(L-N)^2} - \sum_{m=0}^{N-1} \sum_{n=0}^{N-1} J_{i+m,j+n} \right]^2 \right\}^{1/2} \tag{1}$$

where L is the number of unit boxes along the edge of the region of interest, N is the mesh size, K is the total number of occupied boxes in the $L \times L$ region, and $J_{i,j}$ is either 0 or 1, depending on whether a box is unoccupied or occupied, respectively. The resulting standard deviation is equivalent to that of Irimura et al. (2) or Melhorn and Packer (3) except for a factor of N or N^2, respectively. In Eqs. 1 and 2 of reference 2, there are two misprints although the calculations appear to have been carried out correctly. The standard deviation, σ, is then normalized by dividing it by σ_r, the average of 10 SD for the same measurement performed on 10 sets of randomly distributed particles at the same density. These sets were constructed by either random placement techniques (15) or by the running of the aggregation program without allowing binding to occur. Note: the latter is necessary to randomize a distribution of particles at densities higher than the density of saturation for the random placement of particles. Also, with the advent of less expensive computing it has been possible to exceed values of the saturation density obtained with the "dart throwing" method (15), a method of random sequential placement where placement attempts are made at random coordinates and a particle is placed if it does not overlap another. A new value for the maximum random packing of discs on a surface generated while producing the data for Table II is a fractional coverage of 0.5455 ± 0.0036.

Values for σ_r are given in Table II. The normalized standard deviation, σ_{N_n}, is then used to generate P, the aggregation parameter by

$$P = \exp\left[\left(\sum_{i=3}^{5} \sigma_{i_n} - 3\right) \frac{\rho}{1.3 \times 10^{-3}}\right]. \tag{2}$$

For 1,600 unit boxes, for the mesh sizes of 3, 4, and 5, it takes 7 s on an IBM 370/168 computing engine running batch, 4.6 s elapsed-time interactive to load data from disk, and process on a PDP 11/60 minicomputer, or 1,255 s on a Hewlett Packard HP85 personal computer that runs interpretive Basic, to load a file from cartridge tape, and process it.

RESULTS

The computer simulation method for the aggregation of particles, described above, produces pictures of particle arrangements as the particles gradually, but irreversibly, join to form clusters of particles, which may in turn join other particles or clusters. The resulting pictures then provide a unique sequence in time, in which the particles indisputably become continually more aggregated. Hence, there is a unique ranking of aggregation pictures, which

TABLE II
AVERAGE VALUES FOR THE STANDARD DEVIATION σ_r OF TEN SAMPLES OF RANDOM PARTICLE DISTRIBUTIONS

Fraction of boxes occupied	Fraction of area covered	Standard Deviation		
		*(3)**	*(4)**	*(5)**
0.01	0.0157	8.8260	15.6860	24.5047
0.02	0.0314	8.6517	15.3719	24.0091
0.03	0.0471	8.4754	15.0546	23.5083
0.04	0.0628	8.2993	14.7376	23.0125
0.05	0.0785	8.1206	14.4153	22.5040
0.06	0.0942	7.9465	14.1038	22.0176
0.07	0.1100	7.7697	13.7854	21.5156
0.08	0.1257	7.5946	13.4702	21.0188
0.09	0.1414	7.4202	13.1579	20.5275
0.10	0.1571	7.2408	12.8360	20.0217
0.11	0.1728	7.0611	12.5119	19.5136
0.12	0.1885	6.8865	12.1990	19.0238
0.13	0.2042	6.7087	11.8808	18.5257
0.14	0.2199	6.5342	11.5675	18.0363
0.15	0.2356	6.3559	11.2466	17.5334
0.16	0.2513	6.1788	10.9300	17.0371
0.17	0.2670	6.0024	10.6140	16.5441
0.18	0.2827	5.8231	10.2945	16.0479
0.19	0.2985	5.6455	9.9768	15.5507
0.20	0.3142	5.4646	9.6512	15.0417
0.21	0.3299	5.2872	9.3332	14.5456
0.22	0.3456	5.1107	9.0179	14.0539
0.23	0.3613	4.9315	8.6990	13.5558
0.24	0.3770	4.7548	8.3820	13.0592
0.25	0.3927	4.5783	8.0677	12.5686
0.26	0.4084	4.4001	7.7486	12.0668
0.27	0.4241	4.2205	7.4266	11.5603
0.28	0.4398	4.0438	7.1105	11.0668
0.29	0.4555	3.8657	6.7891	10.5619
0.30	0.4712	3.6895	6.4706	10.0593
0.31	0.4869	3.5130	6.1520	9.5579
0.32	0.5027	3.3425	5.8447	9.0754

*Mesh size.

has not been previously available. These sequences are then used to evaluate four different methods (described above) for measuring the degree of aggregation. The boxing technique appears to be the most suitable for the electron-microscopy laboratory. The method requires only a transparent ruled sheet and widely available computation facilities. A sample program is shown in the Appendix.

Mean Cluster Size

The mean cluster size must exhibit a monotonic increase with time, starting with one particle per cluster and ending with all particles in a single cluster after sufficient time, because unbinding of particles is not allowed to occur. Since aggregation may be the result of the binding of particles, the cluster size should be representative of the degree to which the binding process has occurred. In Fig. 3, the mean cluster size shows the monotonic behavior expected. Further, the plots of the cluster size vs. time show a behavior that is nearly linear with respect to time. Although this method does require digitizing of the particle locations, the number of computer calculations can be kept fairly low. The computations required increase only as K, the number of particles, increases. The method, since it deals only with the attachment of particles, does not differentiate between globular and stringlike clusters. If it is desirable to consider such differences, the mean cluster size would not be useful.

The Radial Distribution Function

The radial distribution function provides much qualitative information about an aggregation, but it is necessary to interpret this information to make the results useful as a measure. The three-dimensional plot of Fig. 4 shows the radial distribution function plotted as a surface of particle density at a given separation vs. particle separation vs. time. To permit all the features of the distribution to remain visible, hidden line removal was not employed in the plot. The predominant feature in the plot is the peak formed at the binding distance, i.e., between 12 and 13 nm. From the height of the first peak, the radial distribution yields information concerning the amount of binding that has taken place. This peak rises early in time, serving

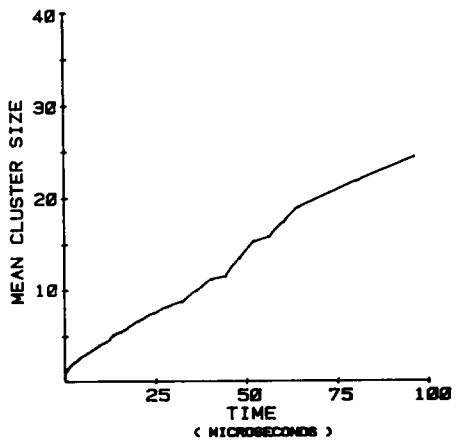

FIGURE 3 Mean cluster size (particles/cluster) vs. time for the run MDS of the aggregation simulation program at a particle density of $\rho = 0.0032$ particles/nm^2.

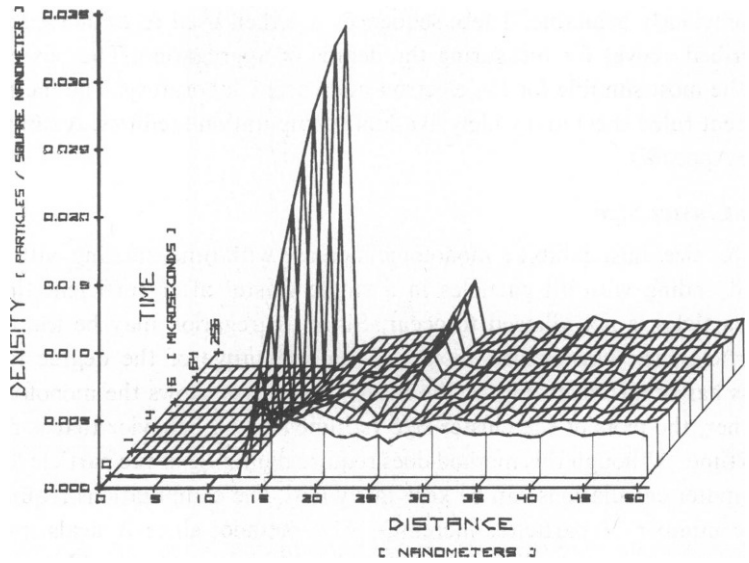

FIGURE 4 Radial distribution surface. The radial distribution function vs. time for run MDS of the aggregation-simulation program run at a particle density of $\rho = 0.0032$ particles/nm^2. Note that the time scale is logarithmic.

to measure overall particle pairing, since every bond between particles will contribute to this peak. The region between 13 and 25 nm reveals some of the structure of the aggregates being formed. The region of zero density at distances below the binding distance shows the effect of the model's hard-core constraint. As the aggregation process continues, there is a valley formed at a distance slightly greater than the binding distance. The valley indicates the situation in which most particles that are in the immediate neighborhood of another particle have been bound to it. Many other properties of the distribution are discernible from the radial distribution surface plotted, but they would be difficult to use as an aggregation parameter. The major drawbacks of the use of the radial distribution function are (*a*) that the input data must be accurately digitized, (*b*) that the method requires considerable computation, increasing approximately as K^2, and (*c*) that the method a simple numerical result from the calculation which would be used as an estimate of aggregation.

Nearest-Neighbor Separations

Nearest-neighbor separations have been used to compare aggregations (4), but working only with the nearest neighbor measures only the number of particle pairs that have formed. The measure of the average distance between the particle centers of nearest neighbors less the binding distance should result in zero when all of the particles are paired. (With the exception of a few holdouts, pairing of particles occurred early in the aggregation simulation.) Thus, while the nearest-neighbor separation provides an excellent measure of the number of particles that have interacted, it does not provide a good measure of the entire aggregation process. Indeed, Fig. 5 shows very little correlation between the average separation and the progression of the aggregation process with time. The time scale was kept the same for the plots throughout: for comparison purposes, and to dramatize the uselessness of the informa-

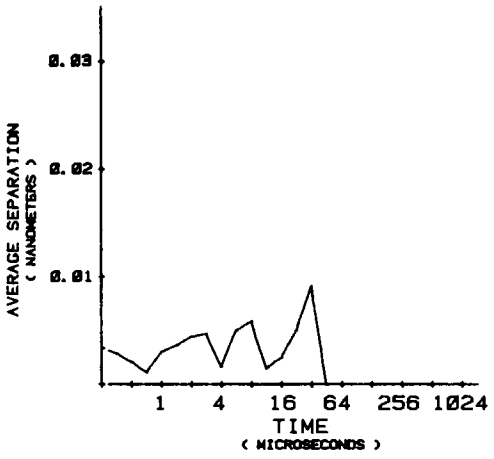

FIGURE 5

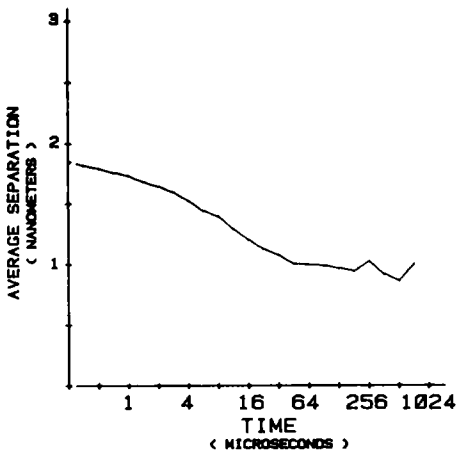

FIGURE 6

FIGURE 5 Average separation of the nearest neighbor for each particle vs. time. The average separation of the nearest neighbors is computed by a program for the data set generated by the program run MDS, an aggregation simulation program run at a particle density of $\rho = 0.0032$ particles/nm^2. Note that the time scale is logarithmic and the separation is taken edge to edge.

FIGURE 6 Average separation of the three nearest neighbors for each particle vs. time. The average separation of the nearest neighbors is computed by a program for the data set generated by the program run MDS, an aggregation-simulation program run at a particle density of $\rho = 0.0032$ particles/nm^2. Note that the time scale is logarithmic and the separation is taken edge to edge.

tion revealed by some of the plots. The plots do not have the monotonic behavior that one would like to see, if the measure is to be of any value. The method offers little more than a signal (the point where the measure intersects the axis and remains zero) indicating that all the particles have interacted. The few particles that remain unbound cause dramatic variations in the average nearest-neighbor separation as they move with respect to the large clusters.

The average separation of the two nearest neighbors offers a function with the desirable feature that it decreases monotonically with respect to time throughout most of the aggregation process, although again after most of the particles have been clustered the few remaining isolated particles and pairs have a substantial effect on the behavior of the curve. Unfortunately, this problem is more than merely an artifact of the computer model. If the method were applied to a highly clustered freeze-fracture, there would be a wide variation in the resulting average separation because of the positions of a few free particles. When using only the two nearest neighbors, chaining of particles would have a dramatic effect on the value of the average separation. A chainlike cluster would have a more pronounced effect than would a globular cluster. Experimenting with the three nearest neighbors for each particle (Fig. 6) produced results that are quite similar to the results for the two nearest neighbors (not shown), although the measure would now be more responsive to the globular cluster than to chainlike clusters. The results at higher densities do not show as much change as the comparable case for the two nearest neighbors. When four nearest neighbors were used, a simular curve was produced, although a few new features emerged. The curves remained flat or even rose slightly after $t = 0$. The study was conducted for up to six nearest neighbors,

because it is possible to pack six discs in the vicinity of another disc in two dimensions. Using four, five, or six nearest neighbors produced no advantage over the use of three nearest neighbors. Although only two typical plots are shown here, plots for each of the nine program runs and 1, 2, 3, 4, 5, and 6 nearest-neighbor separations were made, i.e., a total of 54 cases. As density increases, the curves approach a horizontal line from which little valuable information can be gathered. The plots of the nearest-neighbor separations all either fluctuate wildly or reach zero early in the aggregation process, when the pairing of the particles is complete.

The calculation of the nearest-neighbor separation has little to offer the electron microscopist as a method for measuring aggregation, particularly since the data must be digitized. The results obtained for the average separation of the three nearest neighbors, Fig. 5, might be used as a parameter to evaluate an aggregation were it not possible for a few lone particles to substantially perturb the average separation.

Boxing Technique

The boxing technique, which measures the normalized standard deviation sampling windows of various sizes, seems to offer the best prospect for a useful measure. The plots of Figs. 7–10 show the normalized standard deviation of the counts in the boxes vs. mesh size vs. time. Note that time is plotted on a logarithmic scale. Fig. 7 shows plots for a random initial positioning of the particles at a fairly low density, $\rho = 0.0021$ particles/nm^2. For all mesh sizes, there is a fairly steady rise with time in the deviation with a more rapid rise early in time at the lower mesh sizes. As one might expect, the larger mesh sizes do not deviate greatly until the aggregation has progressed substantially. In Fig. 8, the density is increased to $\rho = 0.0032$ particles/nm^2. Again the behavior is as expected, i.e., the deviation increases steadily with

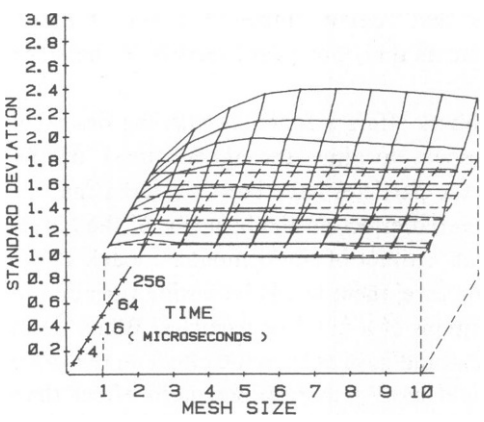

FIGURE 7

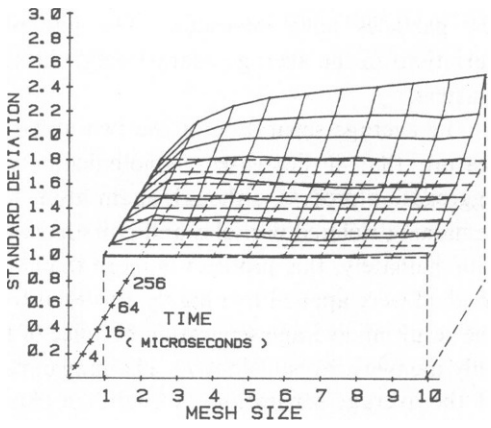

FIGURE 8

FIGURE 7 Normalized standard deviation vs. mesh size vs. time. Results of the boxing method applied to the program run LDS. Particle density was $\rho = 0.0021$ particles/nm^2. The particle positions were initially random. Note that the time scale is logarithmic.

FIGURE 8 Normalized standard deviation vs. mesh size vs. time. Results of the boxing method applied to the program run MDS. Particle density was $\rho = 0.0032$ particles/nm^2. The particle positions were initially random. Note that the time scale is logarithmic.

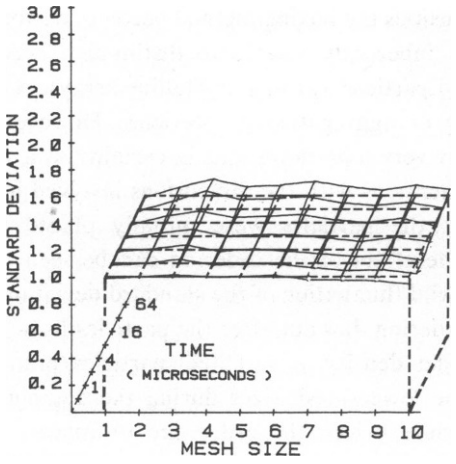

FIGURE 9

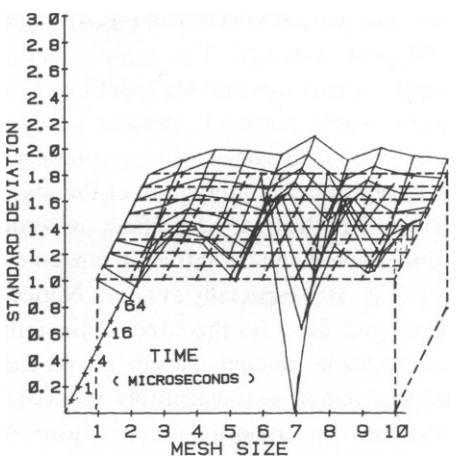

FIGURE 10

FIGURE 9 Normalized standard deviation vs. mesh size vs. time. Results of the boxing method applied to the program run HDS. Particle density was $\rho = 0.0043$ particles/nm^2. The particle positions were initially random. Note that the time scale is logarithmic.

FIGURE 10 Normalized standard deviation vs. mesh size vs. time. Results of the boxing method applied to the program run HDU. Particle density was $\rho = 0.0043$ particles/nm^2. The particle positions were in a square lattice. Note that the time scale is logarithmic.

time for all of the mesh sizes. The slower early increase in the deviation at the larger mesh sizes is less apparent at this density than at the lower density, due in part to the more rapid clustering occurring at this higher density. In Fig. 9 (again having randomly placed particles for the initial condition), the density of the particles has been increased to $\rho = 0.0043$ particles/nm^2, corresponding to the reported density on the human erythrocyte (11). The high density no longer permits much deviation in the counts for a given mesh size. Clearly, less variation is seen in the counts for any of the mesh sizes >3, compared with the Figs. 7 and 8. The fact that there can be little variation, diminishes the usefulness of the method as the density increases. The boxing technique, which measures the fluctuation of the local particle densities, may be related to what one observes visually in an electron micrograph as patchiness or open spaces. Hence, one can understand the limitation that occurs as the density moves in the direction of saturation (i.e., the highest density for which a random placement of particles can be made) or even approaches the close-packing density. As the saturation density is approached, the particles aggregate much sooner because of their proximity. (It is interesting to note that the human erythrocyte has a particle density close to the saturation density of discs of the same diameter (12.5 nm) as the binding distance of the particles. This is consistent with a model of membrane biogenesis in which particles are inserted into the membrane when it is still fluid, i.e., at the reticulocyte stage at the latest. The close-packed ordered arrays observed in some membranes might simply be explained by a systematic attraction force between particles that are mobile in the membrane. In a random arrangement of particles at densities that approach saturation, many of the particles will be quite close to one another. As the density increases, the space that can be vacated by the particles is drastically reduced. Hence, one would expect much less fluctuation in the local particle densities than is observed

at the lower particle densities. Thus, at higher densities the boxing method becomes perforce a less effective measure. The boxing method is inherently unable to distinguish between clustering of particles and the ordering of isolated particles (as in a crystalline array). A high deviation would normally indicate a clustering or aggregation of particles. However, an ordered array of particles will also produce many very high deviations in certain mesh sizes. This depends on the interaction of the mesh dimensions with the dimensions involved in the ordering. To illustrate the effect of ordering, the particles were initially placed in a two-dimensional square lattice arrangement. The effect of the ordering can be seen quite clearly (Fig. 10), especially at $t = 0$. Notice the wild fluctuation of the standard deviation. At the two lower densities the effect of the initial ordering dies out after the particles have been permitted some random movement. At the higher density, $\rho = 0.0043$ particles/nm^2, this initial fluctuation is considerably reduced in the lower mesh sizes during the aggregation process, but the majority of the clustering occurs before the order can disappear. This phenomenon can be observed in Fig. 10, but was also evident visually in plots of the positions of the particles similar to the plots of Fig. 1. Therefore, to make the method useful one must find a means to compensate for the possible ordering of the particles. If the boxing technique is applied to a distribution where the particle density gives a fractional coverage (the fraction of the area of observation covered by the area of a disc of diameter B times the number of particles K) of <0.58, Eq. 2 has been found to generate a single parameter, P, describing the aggregation state. The method yields good results if the ordering factor, F, defined as

$$F = 40 \sum_{i-3}^{5} \left[\left(\sum_{j-3}^{5} \frac{\sigma_{j_n}}{3} \right) - \sigma_{i_n} \right]^2 \tag{3}$$

where σ_{N_n} is again the normalized standard deviation for a mesh size, N, is not >1. A plot of the parameter, P, vs. time is given (Fig. 11). The behavior of the parameter with time is quite similar to that of the mean cluster size (Fig. 3).

There are some serious difficulties with the method as the density increases, since there is

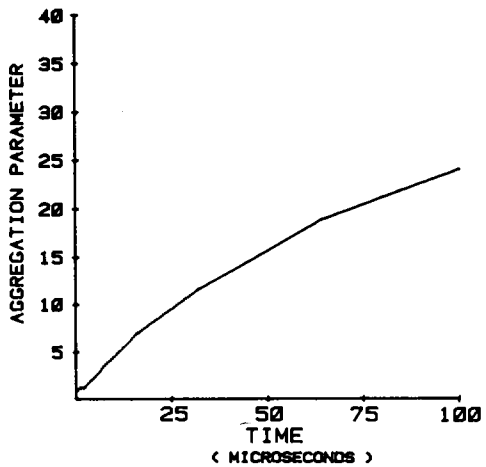

FIGURE 11 Aggregation parameter vs. time. Resulting parameter, P, from the boxing method, which was applied to the program run MDR.

less available space for vacant patches to occur. Also, there is a problem distinguishing between ordering and aggregation of particles. The time required to run the program for various mesh sizes increases as the square of the mesh size, and little seems to be gained by extending beyond the first six mesh sizes. The principal advantage of the boxing method is that the necessary accuracy of the digitization is reduced from the particle positions to very much coarser digitization. The unit box in which each particle lies is determined, rather than the particle's exact position. For mesh sizes of 2–5, the results compare well with the aggregation that takes place (Figs. 7–10).

PRACTICAL APPLICATION OF THE BOXING METHOD The method is applied to an electron micrograph as follows:

(*a*) draw a grid (as described above) on a transparent ruled sheet (the same grid may be used for any micrograph at the same enlargement), a 40 × 40 grid is convenient and sufficient.

(*b*) Write in an appropriate place a "1" for each particle. (It may be convenient to use the boxes on a coding form corresponding to the coordinates of the unit box occupied by the particle.)

(*c*) Prepare the data for the computer, using a program similar to that in the Appendix. The computer will return values for P, the aggregation parameter; F, the ordering factor; and the values of σ_n.

(*d*) Run the computer program. Step (*b*) takes approximately 45 minutes, with little or no experience, for a fraction coverage of 0.5 on a 40 × 40 mesh. Step (*d*) takes ~7 s on an IBM 370/168 computer, 4.6 s on a PDP 11/60 minicomputer, and about 1,255 s on a Hewlett-Packard 85 personal computer.

RESULTS OF APPLICATION The method was applied to three electron micrographs of intramembranous particles from human erythrocyte ghosts. To verify good self correlation of the results of the method, three grids were placed on tracings of each of the electron micrographs. The outlines of the grids on each image are shown in Fig. 1.

The results of the application of the method are shown in Table III. The values for the ordering factor, F, show that tracing *b* of Fig. 1 has more order than the others, probably because of its lower density and a couple of vacant areas. None of the results show sufficient ordering to question the validity of the result.

TABLE III
RESULTS OF AGGREGATION MEASUREMENTS

Tracing	Grid	Density	Aggregation	Ordering
		particles/nm²	*P*	*F*
a	1	0.0020	4.683	1.242
a	2	0.0019	4.626	1.199
a	3	0.0020	3.572	0.911
b	1	0.0018	7.191	3.355
b	2	0.0019	7.247	2.287
b	3	0.0018	6.923	2.180
c	1	0.0021	7.722	1.150
c	2	0.0020	6.262	1.466
c	3	0.0021	6.884	1.522

While the level of clustering is fairly low in the three tracings, even the subtle difference in the degree of aggregation between *a* and *b* (Fig. 1) can be distinguished. Despite the low clustering (roughly comparable to cluster sizes of 3–6 particles/cluster on the average) the clustering is substantially greater than the generated random distributions used to produce Table II, which of course would have an average value of $P = 1.0$.

CONCLUSION

If digitizing equipment is available to the electron microscopist, then the particle positions on the sample electron micrographs can be determined accurately and some useful information can be derived from an analysis of the mean cluster size and the nearest-neighbor separations. The nearest neighbor separations for the two and three nearest neighbors reveal information about the nature of the clusters. All of the methods, with the exception of the mean cluster size analysis exhibit a dramatic dependence on the particle density, and tend to fail as aggregation measures when the density of the particles increases much beyond the saturation density for random placement of particles.

Despite the problem of ordering and the difficulties that occur as the density increases (which are relevant only for certain membranes of very high particle density) the boxing technique is a viable method requiring far less equipment (only a transparent ruled sheet and some computation facilities) for evaluating electron micrographs than the other methods discussed. Hence, the boxing technique would be the method of choice for establishing a single, simple parameter to describe an aggregation.

Received for publication 10 November 1980 and in revised form 28 April 1981.

APPENDIX

```
      DIMENSION SIG(6),SIGN(6),SIGR(6),JJ(80,80)
      INTEGER O
      DATA O /'O'/
      READ(5,5)NB
      READ(5,6)((JJ(I,J),I=1,NB),J=1,NB)
      NP=0
      DO 1 I=1,NB
      DO 1 J=1,NB
      IF(JJ(I,J).FQ.O)NP=NP+1
    1 CONTINUE
      AR =(NB*0.707*12.5)**2
      RHO=NP/AR
      SIGR(3)=0.7982
      SIGR(4)=0.9904
      SIGR(5)=1.1218
      DO 4 NN=3,5
      RI=FLOAT(NN*NN*NP)/FLOAT(NB*NB)
      SI=0.0
      NB1=NB+1-NN
      DO 3 I=1,NB1
      DO 3 J=1,NB1
      KK=0
```

```
      DO 2 M=1,NN
      DO 2 N=1,NN
      K=I+M-1
      L=J+N-1
      IF(JJ(K,L).NE.O) GO TO 2
      KK=KK+1
    2 CONTINUE
      SI=SI+(RI-FLOAT(KK))**2
    3 CONTINUE
      SIG(NN)=SQRT(SI/FLOAT(NB1*NB1-1))
      SIGN(NN)=SIG(NN)/SIGR(NN)
    4 CONTINUE
      WRITE(6,10)(SIG(I),SIGN(I),SIGR(I),I=1,5)
      P=EXP(RHO*(SIGN(3)+SIGN(4)+SIGN(5)-3.0)/0.0013)
    5 FORMAT(I2)
    6 FORMAT(40A1)
    7 FORMAT(' P = ',F8.3,' F = ',F10.4,' NSD3 =',F8.5,
     1' NSD4 =',F8.5,' NSD5 =',F8.5,' NP =',I5,' RHO =',F7.4,' NB =',I3)
      S=0.0
      DO 8 J=3,5
    8 S=S+SIGN(J)
      S=S/3.0
      F=0.0
      DO 9 I=3,5
    9 F=F+(S-SIGN(I))**2
      F=F*40.0
      WRITE(6,7)P,F,SIGN(3),SIGN(4),SIGN(5),NP,RHO,NB
   10 FORMAT(3F12.5)
   11 FORMAT(60(1X,A1))
      DO 12 I=1,NR
      WRITE(6,11)(JJ(I,J),J=1,NB)
   12 CONTINUE
      STOP
      END
```

REFERENCES

1. Rash, J. E. and C. S. Hudson. 1979. Freeze-Fracture: Methods, Artifacts, and Interpretations. Raven Press, New York. 204 pp.
2. Irimura, T., M. Nakajima, H. Hirano, and T. Osawa. 1975. Distribution of ferritin conjugated lectins on sialidase treated membranes of human erythrocytes. *Biochim. Biophys. Acta.* 413:192–201.
3. Melhorn, R. J. and L. Packer. 1976. Analysis of freeze fracture electron micrographs by a computer-based technique. *Biophys. J.* 16:613–625.
4. Copps, T. P., W. S. Chelack, and A. J. Petkau. 1976. Variation in distributions of membrane particles in *Acholeplama laidlawii B* with pH. *J. Ultrastruc. Res.* 55:1–3.
5. Abbas, A. K., K. A. Ault, M. J. Karnovsky, and E. R. Unanue. 1975. Nonrandom distribution of surface immunoglobin on murine B lymphocytes. *J. Immunol.* 114:1197–1204.
6. Romano, E. L., C. Stolinski, and N. C. Hughes-Jones. 1975. Distribution and mobility of A, D, and C antigens on human red cell membranes: studies with gold labelled antiglobulin reagent. *Brit. J. Hematol.* 30:507–516.
7. Weinstein, R. S. 1976. Changes in plasma membrane structure associated with malignant transformation in human urinary bladder epithelium. *Cancer Res.* 36:2518–2524.
8. Elgsaeter, A., and D. Branton. 1974. Intramembrane particle aggregation in erythrocyte ghosts. *J. Cell Biol.* 63:1018–1030.
9. Pielou, E. C. 1977. Ecology. John Wiley & Sons, New York.

10. Donnell, J. T. 1981. Thesis. Drexel University, Philadelphia, Pa.
11. Finegold, L. X. 1976. Cell membrane fluidity: molecular modeling of particle aggregation seen in electron microscopy. *Biochim. Biophys. Acta.* 448:393–398.
12. Perelson, A. S. 1978. Spatial distribution of surface immunoglobulin on B lymphocytes. *Exp. Cell Res.* 112:309–321.
13. Gershon, N. D., A. Demsey, and C. W. Stackpole. 1979. Analysis of local order in the spatial distribution of cell surface molecular assemblies. *Exp. Cell Res.* 122:115–126.
14. Pearson, R. P., S. W. Hui, and T. P. Stewart. 1979. Correlative statistical analysis and computer modelling of intramembraneous particle distributions in human erythrocyte membranes. *Biochim. Biophys. Acta.* 557:265–282.
15. Finegold, L., and J. T. Donnell. 1979. Maximum density of random placing of membrane particles. *Nature (Lond.).* 278:443–445.